Visualization of the gas flow in fuel cell bipolar plates using molecular flow tagging velocimetry and micro PIV

Christian Hecht[1], Nadine v. d. Schoot[2], Helmut Kronemayer[1], Ralph Lindken[2], Christof Schulz[1]

1: IVG and CeNIDE, University of Duisburg-Essen, Duisburg, Germany, Christian.Hecht@uni-due.de
2: ZBT, Center for Fuel Cell Technology, Duisburg, Germany

Abstract Main components of proton exchange membrane fuel cells are bipolar plates that electrically connect the electrodes and provide a gas flow to the membrane. We investigate the flow in the channel structures of the bipolar plates. Flow tagging is used to visualize the propagating and mixing gas stream. It is shown that a part of the gas convects perpendicularly to the channel structure. An analysis of the diffusion compared to the convection shows different mixing behavior for both flow directions. Additionally, the flow field is investigated in detail near the channel wall using Micro PIV in a Reynolds-Number-scaled liquid fluid system. For a more exact comparison of the experimental setups, flow tagging in both gas and liquid systems are performed.

1. Motivation

Fuel cells are a promising technology for clean energy conversion from different primary sources. Fuel cells can be regarded as batteries with a constant influx of reaction gas. One approach is the proton exchange membrane (PEM) fuel cell, where hydrogen and oxygen react to form water in the membrane electron assembly (MEA). The MEA consists of the membrane with a catalyst coating and a porous gas diffusion layer (GDL) on both sides. The performance and the operation stability of a fuel cell depend directly on the homogenous supply of the MEA with fresh gases (Mehta and Cooper 2003). For this purpose, the MEA does not only electrically contact the electrodes but also transports gas in the gas diffusion layer (GDL) to and from both the anode and cathode. Current interest is on the optimization of the transport through these structures. Therefore, non-intrusive measurements of the flow field inside fuel cells are necessary for the optimization of such devices.

In this work, two techniques are employed to study the flow and transport phenomena in the flow field. Micro-Particle Image Velocimetry (Micro-PIV) allows to measure local velocity distributions with high spatial resolution. The method is usually applied to liquid flows. The application to gas flows is under development (van der Schoot et al. 2010; Burgmann et al. 2010). In this experiment the gas flow is replaced by a liquid (Martin et al. 2005, Barreras et al. 2008). Similar fluid dynamic conditions are achieved by Reynolds-number scaling. The working fluid water contains fluorescent particles which are imaged in two subsequent time steps and the velocities are calculated from their displacement.

Alternatively, the global transport process is observed as a function of time using flow tagging. This method allows to observe about how gases distribute and whether "short-cuts" are present in the flow field that might lead to an inhomogeneous distribution of fresh gases to the active layer. In the fuel cell application this might lead to a local undersupply and drying of the MEA, local temperature increase and degradation of the cell.

Fig. 1: Photograph of the sealed bipolar plate with optical access to the flow field, with inlet at the bottom right corner and outlet at the top left corner.

2. Setup and Techniques

For the laser-optical measurements an optically accessible fuel cell model was built with a bipolar plate, a fused silica cover plate and inlet- and outlet connectors. To keep the plate gas tight, it was sealed using a silicon gasket. The gasket also serves as a spacer that creates a gap of approximately 100 µm between the bipolar plate with the channel structure and the cover window. This gap is designed to simulate the gas flow through the gas diffusion layer, which in this setup must be replaced to provide optical accessibility. Fig. 1 shows a photograph of the
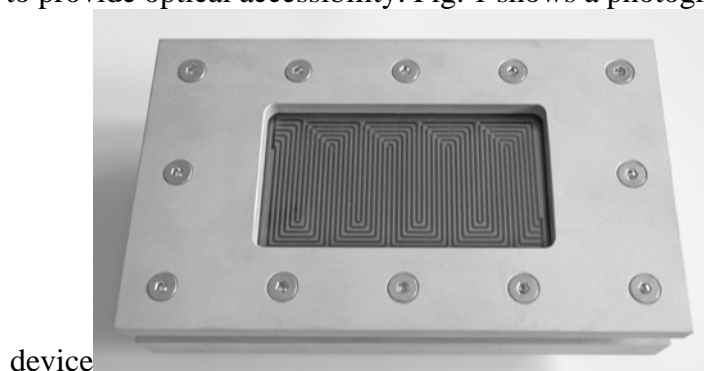

device

Fig. 1. The gas inlet is at the lower right corner at the back side of the plate, while the outlet is at the upper left one (not visible in the picture).

In recent works (Koochesfahani et al. 2001, Roetmann et al. 2008) molecular flow tagging has been applied succesfully for the diagnotics of micro fluid systems. Flow tagging can in principal be performed in two ways. A species that can be detected by laser-induced fluorescence is either locally generated by optical methods or added to the flow, e.g. by a pulsed valve. The transport of the generated feature than allows to determine velocity information as well as information about mixing by diffusion and local dispersion in flow velocities. Optical generation of observable species has been shown by vibrational excitation of O_2 (Miles et al. 1987) photolysis of hot water forming OH (Boedecker, 1989), nitric dioxide (Orlemann et al. 1999) or N_2/O_2 mixtures (van der Laan et al. 2003) forming NO. with these line structures, local velocities or velocity fields have been observed. When suddenly changing the flow composition by adding a fluorescent species, eg. Acetone (Lozano et al., 1993) or NO (Grünefeld et al. 1998) the transport of the resulting step function and the change in the slope of the concentration increase can be used to derive average effective velocities that can be directly related to the combined tranport effects that are relevant for the fuel-cell application.

In the flow tagging approach used in this work, we add NO to the fresh gases by suddenly switching from an NO-free to a NO containing Argon flow. Additional experiments that attempted to locally generate NO from the photolysis of NO_2 failed because the required laser fluence exceeded the damage threshold of the bipolar plate, thus causing rapid fouling of the front window. The working fluid is argon, while the fuel cell is operated with hydrogen. The self-diffusion coefficient of argon is 0.24×10^{-4} m²/s, while the self-diffusion coefficient of hydrogen is 1.7×10^{-4} m²/s (Winkelmann 2007, Al'zhanov et al. 2003). The difference in diffusion coefficients of less than one order guarantees the comparability of the Ar model with the H_2 flow. For the excitation of the NO molecule, the first anti-stokes line of a Raman-shifted KrF excimer laser (Lambda EMG 150) at $44395 cm^{-1}$ was used based on transitions outlined (Bessler et al. 2002). A beam homogenizer helped to generate a homogeneously illuminated area ox 100 x 50 mm². The resulting fluorescence signal is detected with an ICCD Camera (LaVision Imager Intense + IRO, equipped with a 105 mm lens) in a two-dimensional imaging back-scatter geometry. The signal is discriminated against elastic scattering with two longpass filters (230 nm) and a bandpass filter (230–250 nm) formed from four high reflecting dielectric mirrors coated for maximum reflection in the given wavelength range.

In order to create a propagating NO front, a pulsed valve was used. To avoid errors resulting from slight pressure variations when opening the valve, t and the pressure on the NO side is controlled. Using a delay generator (Stanford Systems) the timing between the opening of the valve and a camera/laser system can be varied and the transport of the NO front was observed in a phase-sampling mode. For each delay, 100 measurements were taken and the resulting LIF signal was averaged. All images were corrected for background, laser pulse energy and beam profile to measure a semi-quantitative signals. After purging the flow field with NO-seeded flow a reference condition was measured. Because of constant temperature, pressure and bath gas composition the measured signal after correction for the local variation in laser fluence is proportional to NO concentration. Comparing the measured signal with the zero and the reference case allows to quantify the relative concentration.

For the micro-PIV measurements we use water as working medium applying velocity scaling. Based on the principle of Reynolds number similarity, the dynamics of a liquid flow and gas flow with the same Reynolds number are supposed to be equivalent. PIV is based on two laser-illuminated images of the seeded flow that are acquired at successive time instants, separated by time interval dt. Each image is scanned into a series of interrogation windows. For each interrogation window, the intensity pattern within the window is cross-correlated between an image pair. The cross-correlation peak within this window corresponds to an average displacement of the seeding particles, and using the time interval dt, provides an average velocity for the particles within this interrogation window. A velocity field can be constructed by cross-correlating the full series of interrogation windows within an image pair. For recent reviews of the method the reader is refered to Wereley and Meinhart (2009) and Lindken et al. (2009). The principle of the micro-PIV method is shown in Fig. 2 (left).
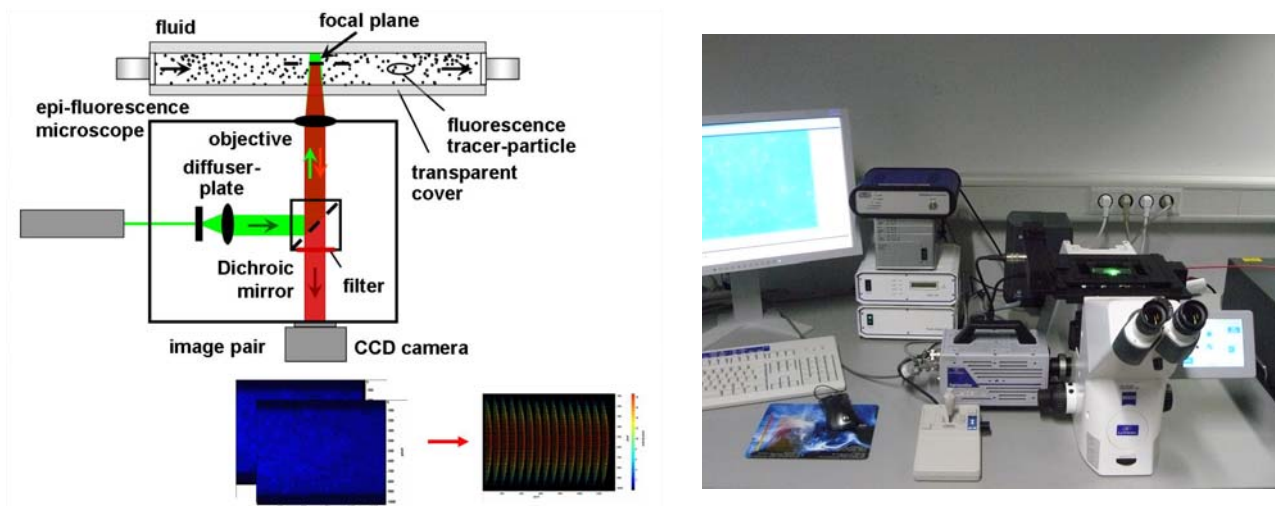
Fig. 2: (left) Schematic micro-particle image velocimetry method. The flow is illuminated by an expanded laser beam, the camera takes pictures with fluorescence filter of seeded fluid.
(right) Micro-PIV experimental setup with an inverse epifluorescence microscope, high-speed laser and camera.

There are some differences between a micro-PIV and the classical PIV application. The classic macroscopic PIV uses double pulse light sheet illumination and the Mie-scattered light is detected to display the particles within the *xy*-plane illuminated by the light sheet. In a micro-PIV application, the double-pulse laser typically illuminates the entire volume of the flow channel. The location of the measuring plane on the *z*-coordinate is defined by the depth of focus of the microscope optics. This allows to investigate flows via micro-PIV in channels with diameters smaller than 1 mm. An epi-fluorescence microscope is used and fluorescent particles are added to the flow. Due to the fluorescence, particles with diameters of few nanometers to a few micrometers are detectable. The laser beam (527 nm) stimulates the dye coated particles to emit red fluorescent light. The fluorescent light passes through a filter that subtracts the green laser refraction light. Therefore, the particles within the measuring plane are clearly visible and separated from the background (and those particles in out-of-focus planes). The path of the laser light is directed through the microscope optics and illuminates the fluid in the channels. The emitted fluorescent light from the particles is then directed through the lens and fluorescence filter to the sensor of a CCD camera.

The micro-PIV setup consists of a 12-bit CCD camera with 1376×1040 pixel resolution (LaVision Imager Intense), a Zeiss epi-fluorescence microscope and a double-cavity diode-pumped laser at 527 nm (New Wave Pegasus) with a pulse length of 180ns that is favourable for fluorescence excitation. The setup is shown in Fig. 2 (right).

To estimate the comparability of the results of both measuring methods, molecular flow tagging in gas flow and micro-PIV in water flow, a verification experiment was performed. The molecular flow tagging experiments were repeated with water as working fluid and a fluorescent dye, rhodamine B (Rh B), was used to visualize the flow and the mixing. The Reynolds number of the water flow (620.2 µl/s) was equivalent to the argon flow in the gas flow experiments. The distribution of the influx as a function of time is measured in a comparable way to the NO molecular tagging experiment. First, a constant flow of pure water is established, then the water is replaced with a concentrated solution of Rhodamin B in water. The flow scene is illuminated by a frequency doubled Nd:YAG laser (532 nm) in volume illumination mode and it is observed with a long pass filter (>545 nm) and a CCD camera at 5 Hz frame rate. The regions that are tagged with the fluorescent dye emit light that is captured by the camera and a time lapse of the migration of the influx is recorded. Because of the velocity scaling, the time lapse is on a different scale. The slower

velocity of the liquid flow allows an observation of the transport of the dye front in "real-time". By comparing the tagging measurements in the liquid and the gas phase, errors due to Reynolds number scaling can be estimated.

Previous gas-phase PIV measurements in millimeter-channels of fuel cell models were realized by a few groups and research institutes. All of them used light sheet illumination and measured in transparent model channels in non-operational condition. Grega and Mc Garry (2007) performed detailed measurements of the flow through a scaled up plexiglass model of a fuel cell stack using PIV. The flow was seeded with an oil-based aerosol in air with particle diameters of nominally 1µm. Using the PIV technique, instantaneous flow fields were captured which were then averaged to obtain mean values and velocity statistics. Based on these data, relationships were found between manifold and cell flow distributions. Sugii and Okamoto (2006) used the Micro-PIV technique to investigate the flow in a transparent model of polymer electrolyte fuel cell under non-operational conditions, which consisted of straight 1mm channels. The velocity distribution of the gas flow with Reynolds numbers of 26 and 130 were successfully measured. Yoon et al. (2006) measured gas-phase velocity fields using particle image velocimetry in acrylic millimeter-scale channels with integrated heater and in a PDMS 180° switchback flow model. Two types of seeding particles were used, smoke particles (<1µm) and water droplets (1-8µm). Based upon experimental results, particles smaller than 1µm are required in order to accurately follow the flow in regions of rapid deceleration.

3. Results and Discussions

Fig. 3 shows the distribution of NO 70 ms after the injection. The inlet valve which is located at the bottom right corner of the image just outside the illuminated area; the outlet is on the top left. There are two main paths for the flow inside the structure. One part of the gas follows the channel structure on the bipolar plate, while another part flows perpendicularly to the channels through the gap between bipolar plate and window.
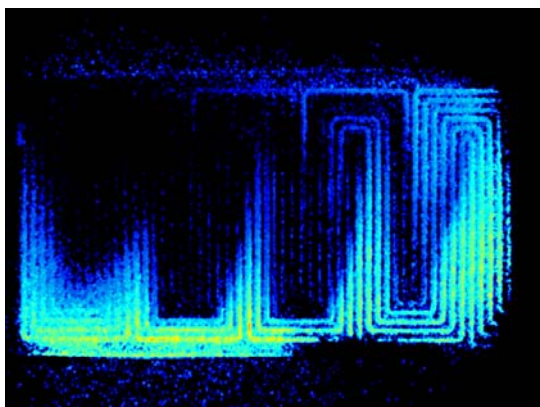

Fig. 3: Distribution of NO in the channel structure 70ms after injection. The inlet is at the lower right corner, the outlet at the upper left. Channel structure is 50 x 100mm

The velocity of the seeded flow parallel to the channel structure shows a decline along the channel length as it would expected due to the perpendicular flow. For 500 sccm argon, a flow velocity of 1.75 m/s is expected, if all of the gas would go through the channels. The measured speed is 1.23 m/s at the beginning of a channel after the first U-shaped corner and 0.29 m/s at the end of a channel near the second corner. Fig. 4 shows, that the loss of velocity is nearly linear along the channel. A comparison with the liquid system shows that, while the overall flow pattern is similar, a quantitative comparison of the detailed behavior in the channels is not successful. The cross talk

between neighboring channels is less compared to the gas system. This result is explained with difficulties in the reproducibility in the experimental setup for the liquid and gas system, mainly in the exact size of the gap between bipolar plate and quartz plate. As a consequence, we are only able to compare the two techniques qualitatively.
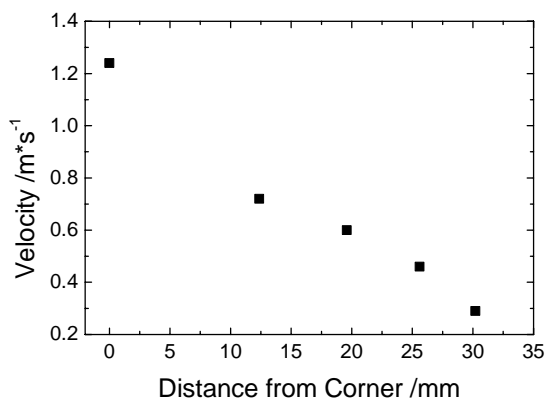

Fig. 4: Velocity of the gas front after first U-shaped corner

Fig. 5 shows the time dependence of the pulse of NO for the top right (only flow through the channels) and the lower left (no flow through the channels) corner. The starting time and maximum intensity are normalized. While the signal of the flow perpendicular to the channel structure rises sharply, the one from the in-channel movement has first a weak increase due to diffusion of the gas and then a stronger increase due to convection. By calculating the beginning time of the convective and diffusive part the time shift between both can be obtained.
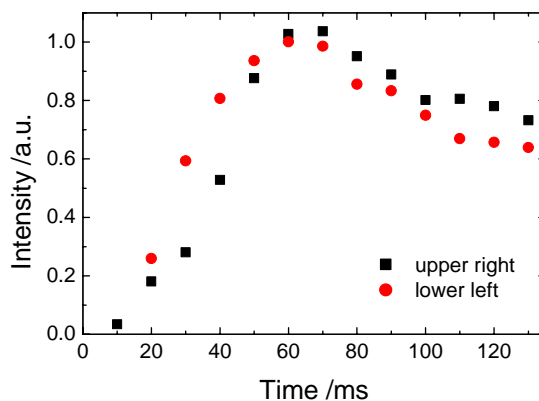

Fig. 5: Time resolved NO distribution at two points of the channel plate where in-channel (black) or out of channel (red) transport dominates

Using the Taylor hypothesis, assuming that the convective flow velocity at one point is constant, a diffusion length is calculated for several points using the velocities from Fig. 4. It can be seen that the diffusion length increases for the flow along the channels, while it decreases perpendicular to the channels resulting in the disappearance seen in Fig. 5. The diffusion constant calculated from the increase is in a range of $6–13\times10^{-7}$ m²/s compared to a value of 3.8×10^{-7} m²/s calculated using the equations from (Hirschfelder et al. 1954). The decrease of the diffusion length perpendicular to the channels shows, that convective mixing due to the steps from the channels dominates over the diffusive mixing.

The measurements show that combination of a porous gas diffusion layer (GDL, here represented by a gap) and the serpentine channel structure has an additional effect compared to the well-known diffusive transport from the channel structure to the parts of the membrane that are covered by the conducting land, i.e. the region between consecutive channel walls. In combination with the serpentine geometry there is a pressure-driven transport through the gap between neighboring channels. If the main transport mechanism would be Diffusion driven, the time scale calculated from the measured Diffusion constants would be in an order of 5 s/mm. In this experiments, in one timestep of 10 ms, the gas transports over a gap region of 15 mm length and over a length of 45 mm in the channels. This leads to a convective time scale of 0.67 ms/mm in the gap and of 0.22 ms/mm in the channel. It should be kept in mind, that due to the rather poor time resolution of 10 ms, the number is affected by a rather large error. Correspondingly Péclet numbers $Pe = l\, v\, /\, D$ (with the characteristic length scale l, here the gap height and the channel diameter, the average velocity v in gap or channel and the diffusion constant $D = 4 \times 10^{-7}$ m^2/s) are $Pe_{gap} = 400$ and $Pe_{channel} = 10000$. The analysis shows that the transport in the gap as well as the transport in the GDL (here represented by a gap) is dominated by convection The convective transport increases mixing and supports homogeneous distribution of gases needed for the efficient operation of the fuel cell, Convective mixing at the bottom of the bipolar plate (on our figures), increases the constant supply of oxygen by mixing gas containing water created from reactions inside the cell with gas containing no water to increase the overall homogeneity of the oxygen distribution.

For the explanation of the effects observed in the flow tagging experiments the flow perpendicular to the channel structure is observed by means of micro-PIV in a measurement plane in the gap and the top side of the channels next to the glass plate. Fig. 66 shows that the main flow inside the channels has a direction along the channels. Between the channels the white streamlines show the bypass flow over the channel wall. Velocities in the gap are 6.5 times smaller than in the channel A small perpendicular gradient appears, while above it the main movement is completely perpendicular to the channels.
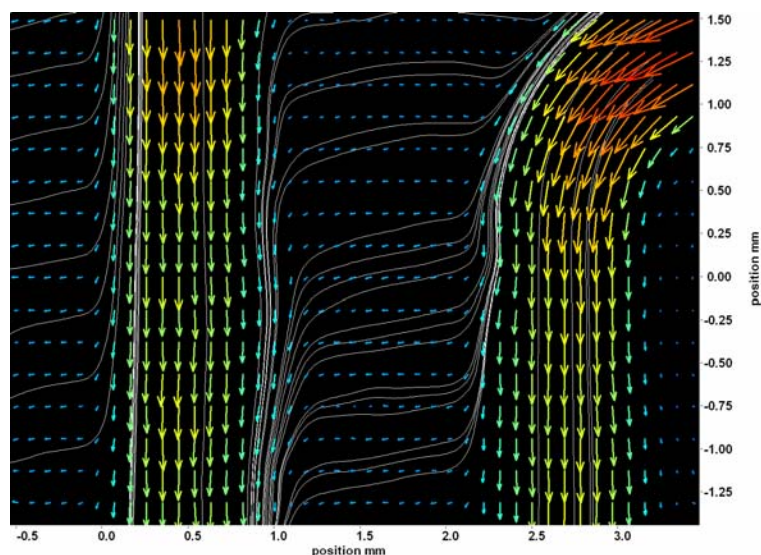

Fig. 6: Velocity distribution and streamlines from micro-PIV measurements in two parallel 1 mm channels with co-flow in the flow field plate.

4. Conclusion

The combination of liquid and gas phase laser-based techniques give a more complete description of the transport inside a bipolar plate. By obtaining combined data it will be possible to have a modeling system that helps understanding the processes. One step further flow tagging can be

applied to optical accessible "real-life" fuel cells, to see the influence of the gas diffusion layer (GDL) on the flow perpendicular to the channels

On the other hand PIV yields quantitative information with high spatial resolution. Further development of the micro-particle image velocimetry (micro-PIV) method for the application in the gas phase will also enable the analysis of gas flow in "real-life" fuel cells (van der Schoot et al. 2010, Burgmann et al. 2010).

6. References

Al'zhanov KZ, Musenov KK (2003)ayandamalary Kazak. Resp. Ulttyk Gylym Akadem 32–38.

Barreras F, Lozano A, Valino L, Mustata R, Marin C (2008) Fluid dynamics performance of different bipolar plates Part I. Velocity and pressure fields. Journal of Power Sources 175:841-850

W. G. Bessler, C. Schulz, T. Lee, J. B. Jeffries, and R. K. Hanson (2002)., "Strategies for laser-induced fluorescence detection of nitric oxide in high-pressure flames. I. A-X(0,0) excitation," Appl. Opt. **41,** 3547-3557

Burgmann S., van der Schoot N, Asbach C, Wartmann J, Lindken R (2010) Analysis of Tracer Particle Characteristics for Micro PIV in Wall-bounded Gas Flows. MICROFLUIDICS2010/108. Proceedings of the 2nd Euroepan Conference on Microfluidics (µFlu'10), Toulouse, France, 8.10.12.2010.

Garbe CS, Roetmann K, Beushausen V, Jähne B (2007) An optical flow mtv based technique for measuring microfluidic flow in the presence of diffusion and taylor dispersion. Exp Fluids (2008) 44:439–450

Gendrich CP, Koochesfahani MM (1996) A spatial correlation technique for estimating velocity fields using molecular tagging velocimetry (mtv). Exp Fluids 22(1):67–77

Gendrich CP, Koochesfahani MM, Nocera DG (1997) Molecular tagging velocimetry and other novel applications of a new phosphorescent supramolecule. Exp Fluids 23:361–372

Grega L, Mc Garry M (2007) Flow characterization of a polymer electronic membrane fuel cell manifold and individual cells using particle image velocimetry. Journal of Fuel Cell Science and Technology, Vol. 4 272-279

Hirschfelder JO, Curtiss CF, Bird RB (1954) Molecular Theory of Gases and Liqiuds. John Wiley and Sons, New York

Koochesfahani MM (ed) (2000) Molecular tagging velocimetry. Meas Sci Technol 11(9):1235– 1300

Koochesfahani MM, Gendrich CP, Nocera DG (1993) A new technique for studying the lagrangian evolution of mixing interfaces in water flows. Bull Am Phy Soc 38:2287

Koochesfahani MM, Nocera DG (2001) Molecular tagging velocimetry maps fluid flows. Laser Focus World, Los Gartos, pp 103–108

Koochesfahani MM, Nocera DG (2007) Molecular tagging velocimetry. In: Tropea C, Yarin A, Foss J (eds) Springer handbook of experimental fluid mechanics, vol B. Springer, Berlin, pp 362– 382

Lindken, R.; Rossi, M.; Grosse, S. Westerweel, J.: Micro-Particle Image Velocimetry (µPIV): Recent developments, applications, and guidelines. Lab on a Chip, 9:2551-2567, 2009.

Martin J, Oshkai P, Djilali N (2005) Flow Structures in a U-Shaped Fuel Cell Flow Channel: Quantitatice Visualization Using Particle Image Velocimetry. Journal of Fuel Cell Science and Technology 2:70-80

Mehta V, Cooper JS (2003) Analysis of PEM fuel cell design. Journal of Power Sources 114:32-53

Orlemann C, Schulz C, Wolfrum J (1999) NO-flowtagging by photodissociation of NO_2. A new approach for measuring small-scale flow structures. Chem Phys Lett 307:15-20

Roetmann K, Schmunk W, Garbe CS, Beushausen V (2008) Micro-flow analysis by molecular tagging velocimetry and planar Raman-scattering Exp Fluids 44:419–430

Stier B, Koochesfahani MM (1999) Molecular tagging velocimetry (mtv) measurements in gas phase flows. Exp Fluids 26:297–304

Sugii Y, Okamoto K (2006) Velocity measurement of gas flow using micro PIV technique in polymer electrolyte fuel cell, Proceedings of ICNMM2006 96216

van der Schoot N, Asbach C, Wartmann J, Heinzel H, Lindken R (2010) Development of gas-phase micro-PIV for fuel cells investigations. Proceedings of GASMEMS2010-DY07, Les Embiez, France, 5.-10.7.2010.

Wereley S T, Meinhart, C D (2009) Recent advances in micro-particle image velocimetry, Annu. Rev. Fluid Mech. 2010. 42:557–76

Winkelmann, J.: *Diffusion of hydrogen*. Lechner, M.D. (ed.). SpringerMaterials - The Landolt-Börnstein Database (http://www.springermaterials.com). Springer-Verlag Berlin Heidelberg, 2007. DOI: 10.1007/978-3-540-49718-9_28

Winkelmann, J.: *Diffusion of argon*. Lechner, M.D. (ed.). SpringerMaterials - The Landolt-Börnstein Database (http://www.springermaterials.com). Springer-Verlag Berlin Heidelberg, 2007. DOI: 10.1007/978-3-540-49718-9_4

Yoon S Y, Ross J W, Mench M M, Sharp K V (2006) Gas-phase particle image velocimetry (PIV) for application to the design of fuel cell reactant flow channels, Journal of Power Sources 160 1017-1025